



Tracing the source of nitrate enriched in a forested stream during storm events

Weitian Ding¹, Urumu Tsunogai¹, Fumiko Nakagawa¹, Takashi Sambuichi¹, Hiroyuki
Sase², Masayuki Morohashi², Hiroki Yotsuyanagi²

¹ Graduate School of Environmental Studies, Nagoya University, Furo-cho, Chikusa-
ku, Nagoya 464-8601, Japan

² Asia Center for Air Pollution Research, 1182 Sowa, Nishi-ku, Niigata-shi, Niigata 950-
2144, Japan

Corresponding author: Weitian Ding, Email: dingweitian@nagoya-u.jp



1 Abstract

2 To clarify the source of nitrate increased during storm events in temperate forested
3 streams, we monitored temporal variation in the concentrations and stable isotopic
4 compositions including $\Delta^{17}\text{O}$ of stream nitrate in a forested catchment (KJ catchment,
5 Japan) during three storm events I, II, and III. The stream showed significant temporal
6 variation in nitrate concentration, from 24.7 μM to 122.6 μM , from 28.7 μM to 134.1
7 μM , and from 46.6 μM to 114.5 μM during the storm events I, II, and III, respectively.
8 On the other hand, the isotopic compositions ($\delta^{15}\text{N}$, $\delta^{18}\text{O}$, and $\Delta^{17}\text{O}$) of stream nitrate
9 showed a decrease in accordance with the increase in the stream nitrate concentration,
10 from +2.5 ‰ to -0.1 ‰, from +3.0 ‰ to -0.5 ‰, and from +3.5 ‰ to -0.1 ‰ for $\delta^{15}\text{N}$,
11 from +3.1 ‰ to -3.4 ‰, from +2.9 ‰ to -2.5 ‰, and from +2.1 ‰ to -2.3 ‰ for $\delta^{18}\text{O}$,
12 and from +1.6 ‰ to +0.3 ‰, from +1.4 ‰ to +0.3 ‰, and from +1.2 ‰ to +0.5 ‰ for
13 $\Delta^{17}\text{O}$ during the storm events I, II, and III, respectively. Besides, we found strong linear
14 relationships between the isotopic compositions ($\delta^{15}\text{N}$, $\delta^{18}\text{O}$, and $\Delta^{17}\text{O}$) of stream
15 nitrate and the reciprocal of stream nitrate concentrations during each storm event,
16 implying that the temporal variation in the stream nitrate can be explained by simple
17 mixing between two distinctive endmembers of nitrate having different isotopic
18 compositions. Furthermore, we found that both concentrations and the isotopic
19 compositions of soil nitrate obtained in the riparian zone of the stream were plotted on
20 the nitrate-enriched extension of the linear relationship. We conclude that the soil nitrate
21 in the riparian zone was responsible for the increase in stream nitrate during the storm



22 events. In addition, we found that the concentration of unprocessed atmospheric nitrate
23 in the stream was stable at $1.6 \pm 0.4 \mu\text{M}$, $1.8 \pm 0.4 \mu\text{M}$, and $2.1 \pm 0.4 \mu\text{M}$ during the
24 storm events I, II, and III, respectively, irrespective to the significant variations in the
25 total nitrate concentration. We conclude that the storm events have little impacts on the
26 concentration of unprocessed atmospheric nitrate in the stream and thus the annual
27 export flux of unprocessed atmospheric nitrate relative to the annual deposition flux can
28 be a robust index to evaluate nitrogen saturation in forested catchments, irrespective to
29 the variation in the number of storm events and/or the variation in the elapsed time from
30 storm events to sampling.

31

32 **1 Introduction**

33 Nitrate is a representative nitrogenous nutrient in biosphere. Traditionally, forested
34 ecosystems have been considered nitrogen limited (Vitousek and Howarth, 1991). Due
35 to the elevated loading of nitrogen through atmospheric deposition, however, some
36 forested ecosystems become nitrogen saturated (Aber et al., 1989), from which elevated
37 levels of nitrate are exported (Mitchell et al., 1997; Peterjohn et al., 1996). In addition,
38 sudden increase in the concentration of nitrate in response to storm events has been
39 reported in forested streams worldwide (Aguilera and Melack, 2018; Creed et al., 1996;
40 Kamisako et al., 2008; McHale et al., 2002), which further enhanced nitrate export from
41 forested ecosystems.

42 Such excessive leaching of nitrate from forested catchment degrades water quality



43 and cause eutrophication in downstream areas (Galloway et al., 2003; Paerl and
44 Huisman, 2009). Thus, tracing the source of nitrate increase during storm events in
45 forested streams is important for sustainable forest management, especially for those
46 nitrogen-saturated forested ecosystems.

47 As for the source of nitrate that was added to stream during storm events, either of
48 the two possible sources have been assumed in past studies; (1) atmospheric nitrate
49 ($\text{NO}_3^-_{\text{atm}}$) in rainwater originally and being supplied directly to stream water through the
50 overland flow (Kaushal et al., 2011; Sebestyen et al., 2014), and (2) soil nitrate
51 originally and being supplied to stream water by the flushing effects on soils (Creed et
52 al., 1996; Ocampo et al., 2006). Nevertheless, monitoring the variation in nitrate
53 concentration, it is difficult to clarify the primary source of nitrate that increases during
54 storm events.

55 The natural stable isotopic composition of nitrate has been widely applied to clarify
56 the sources of nitrate in natural freshwater systems (Burns and Kendall, 2002; Durka et
57 al., 1994; Kendall et al., 2007). In particular, triple oxygen isotopic compositions of
58 nitrate ($\Delta^{17}\text{O}$) have been used in recent days as a conservative tracer of $\text{NO}_3^-_{\text{atm}}$
59 deposited onto a forested catchment (Inoue et al., 2021; Michalski et al., 2004;
60 Nakagawa et al., 2018; Tsunogai et al., 2014), showing distinctively different $\Delta^{17}\text{O}$ from
61 that of remineralized nitrate ($\text{NO}_3^-_{\text{re}}$), derived from organic nitrogen through general
62 chemical reactions, including microbial N mineralization and microbial nitrification.
63 While $\text{NO}_3^-_{\text{re}}$, the oxygen atoms of which are derived from either terrestrial O_2 or H_2O



64 through microbial processing (i.e., nitrification), always shows the relation close to the
 65 “mass-dependent” relative relation between $^{17}\text{O}/^{16}\text{O}$ ratios and $^{18}\text{O}/^{16}\text{O}$ ratios; $\text{NO}_3^-_{\text{atm}}$
 66 displays an anomalous enrichment in ^{17}O reflecting oxygen atom transfers from
 67 atmospheric ozone (O_3) during the conversion of NO_x to $\text{NO}_3^-_{\text{atm}}$ (Alexander et al.,
 68 2009; Michalski et al., 2003; Morin et al., 2011; Nelson et al., 2018). As a result, the
 69 $\Delta^{17}\text{O}$ signature defined by the following equation (Kaiser et al., 2007) enables us to
 70 distinguish $\text{NO}_3^-_{\text{atm}}$ ($\Delta^{17}\text{O} > 0$) from $\text{NO}_3^-_{\text{re}}$ ($\Delta^{17}\text{O} = 0$):

$$71 \quad \Delta^{17}\text{O} = \frac{1 + \delta^{17}\text{O}}{(1 + \delta^{18}\text{O})^\beta} - 1 \quad (1)$$

72 where the constant β is 0.5279 (Kaiser et al., 2007), $\delta^{18}\text{O} = R_{\text{sample}}/R_{\text{standard}} - 1$ and R is
 73 the $^{18}\text{O}/^{16}\text{O}$ ratio (or the $^{17}\text{O}/^{16}\text{O}$ ratio in the case of $\delta^{17}\text{O}$ or the $^{15}\text{N}/^{14}\text{N}$ ratio in the case
 74 of $\delta^{15}\text{N}$) of the sample and each standard reference material. In addition, $\Delta^{17}\text{O}$ is almost
 75 stable during “mass-dependent” isotope fractionation processes within terrestrial
 76 ecosystems. Therefore, while the $\delta^{15}\text{N}$ or $\delta^{18}\text{O}$ signature of $\text{NO}_3^-_{\text{atm}}$ can be overprinted
 77 by the biological processes subsequent to deposition, $\Delta^{17}\text{O}$ can be used as a robust tracer
 78 of unprocessed $\text{NO}_3^-_{\text{atm}}$ to reflect its accurate mole fraction within total NO_3^- , regardless
 79 of the progress of the partial metabolism (partial removal of nitrate through
 80 denitrification and assimilation) subsequent to deposition (Michalski et al., 2004;
 81 Nakagawa et al., 2013, 2018; Tsunogai et al., 2011, 2014, 2018).

82 In this study, by using the stable isotopes including $\Delta^{17}\text{O}$ of nitrate as tracers, we
 83 clarified (1) the source of nitrate in a forested stream that was added during storm events,
 84 and (2) the temporal variation in the concentration of $\text{NO}_3^-_{\text{atm}}$ in response to storm



85 events. In addition, the impacts of storm events on the index of nitrogen saturation lately
86 proposed by Nakagawa et al. (2018) were discussed.

87

88 **2 Methods**

89 **2.1 Study site**

90 As for the studying field to trace the source of stream nitrate during storm events, we
91 chose Kajikawa forested catchment (KJ catchment) in Japan, in which several past
92 studies had been done to clarify the temporal variation in the concentration of stream
93 nitrate and the status of nitrogen saturation (Kamisako et al., 2008; Nakagawa et al.,
94 2018; Sase et al., 2021). This is a small, forested catchment (3.84 ha) located in the
95 northern part of Shibata City, Niigata Prefecture, along the coast of Sea of Japan (Fig.
96 1a). The KJ catchment predominantly slopes towards the west-northwest, with a mean
97 slope of 36°, and the elevation ranges from 60 to 170 m above sea level (Fig. 1b). The
98 catchment is fully covered by Japanese cedars (*Cryptomeria japonica* D. Don) that were
99 approximately 46 years old in 2018 (Sase et al., 2021). The parent material is
100 granodiorite and brown forest soils (Cambisols) have developed in this area (Kamisako
101 et al., 2008; Sase et al., 2008). The lowest, highest, and mean monthly temperatures
102 recorded at the nearest meteorological station (Nakajo station) were 1.0 °C (in February),
103 27.9 °C (in August), and 14.5 °C, respectively, from 2017/5 to 2020/3. The annual mean
104 precipitation was around 2500 mm, approximately 17% of which occurred during
105 spring (from March to May), approximately 20% during summer (from June to August),



106 approximately 28% during fall (from September to November), and approximately 35%
107 during winter (from December to February). The catchment usually experiences
108 snowfall from late December to March.

109 From 2003 to 2005, Kamisako et al. (2008) determined temporal variation in the
110 concentration of Ca^{2+} , Mg^{2+} , Cl^- , and NO_3^- eluted from the catchment via a stream at
111 intervals of 1 to 3 hour for 2 to 3 days on each and found that significant increase in the
112 stream nitrate concentration during storm events, from less than 30 μM to more than
113 120 μM . On the basis of the observed nitrate enrichment in the stream water, they
114 concluded that atmospheric nitrogen inputs exceeded the biological demand at the
115 catchment and proposed that the KJ catchment was under nitrogen saturation.
116 Nakagawa et al. (2018) determined temporal variation in the concentrations and stable
117 isotopic compositions ($\delta^{15}\text{N}$, $\delta^{18}\text{O}$, and $\Delta^{17}\text{O}$) of both stream nitrate and soil nitrate for
118 two years (from 2012/12 to 2014/12) and concluded that nitrate in the groundwater of
119 the catchment was the major source of nitrate in the stream water during the base flow
120 periods. Additionally, the export flux of unprocessed atmospheric nitrate relative to the
121 deposition flux of atmospheric nitrate in KJ catchment ($M_{\text{atm}}/D_{\text{atm}}$) was larger (9.4 %)
122 than the other catchment they studied simultaneously (6.5 % and 2.6 % respectively)
123 and proposed that the $M_{\text{atm}}/D_{\text{atm}}$ ration can be used as the index of nitrogen saturation.
124 Moreover, Sase et al. (2021) reported the nitrate concentration of the stream has been
125 increasing in recent years, which implies that nitrogen saturation is still ongoing in the
126 forest.

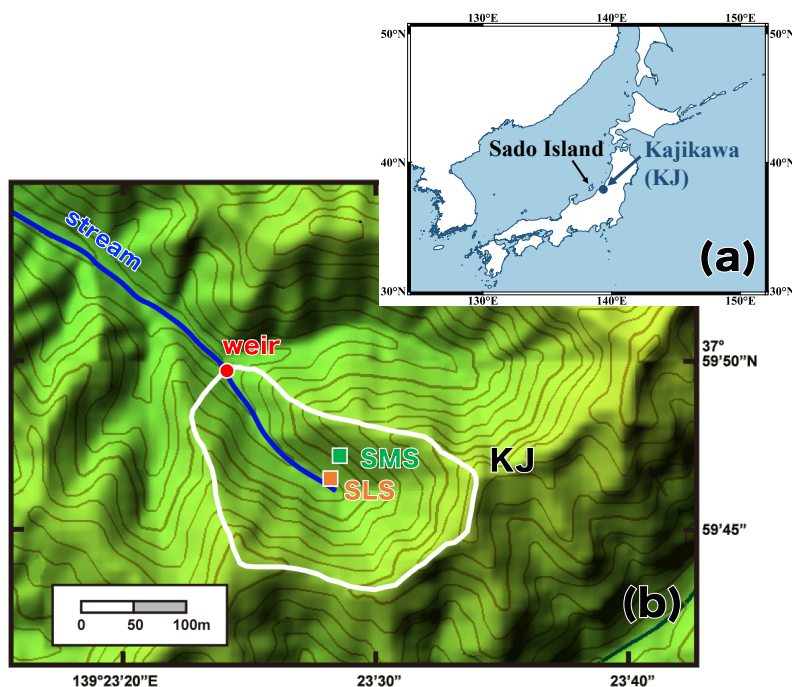


Figure. 1 A map showing the locations of the studied Kajikawa (KJ) catchment in Japan (a) and a colored altitude map of the KJ catchment (b) (modified after Nakagawa et al. 2018). The white line denotes the whole catchment area, and the red circle denotes the position of the weir where the stream water was sampled. The orange (SLS) and green (SMS) circles denote the sampling stations of soil water in the riparian and upland zone, respectively, in the past study (Nakagawa et al., 2018).

2.2 Discharge rates and weather information

A V-notch weir (half angle: 30°) and a partial flume were installed at the bottom of the catchment (Fig. 1b), where the discharge rates were determined. The weather



139 information including the precipitation monitored by Japan Meteorological Agency at
140 the nearest station of KJ catchment (Nakajo station; 38°04'60" N, 139°23'30" E) was
141 used for that in the KJ catchment. Because the accumulated snow was not monitored
142 in Nakajo station, however, those monitored at the Niigata station (37°53'60" N,
143 139°01'10" E) was used instead.

144

145 2.3 Sampling

146 In this study, the concentrations and stable isotopic compositions ($\delta^{15}\text{N}$, $\delta^{18}\text{O}$, and
147 $\Delta^{17}\text{O}$) of stream nitrate eluted from the KJ catchment were monitored every month
148 additionally for more than 2 years (routine observation). Additionally, during storm
149 events, the same parameters were monitored every hour for 1 day (intensive
150 observation). Stream water was sampled at the weir located on the outlet of the KJ
151 catchment (Fig. 1b). Routine observation was performed manually using bottles at the
152 weir approximately once a month from 2017/5 to 2020/3. Intensive observation was
153 conducted during the three storm events I, II, and III (2019/8/22, 2019/10/12, and
154 2020/9/13, respectively), where the water samples were collected at intervals of 1 hour
155 over 24 hours using an automatic water sampler (SIGMA 900, Hach, USA). In this
156 study, 0.5 or 2 L polyethylene bottles washed using chemical detergents were rinsed at
157 least three times using deionized water and dried in the laboratory before being used to
158 store the water samples.

159



160 2.4 Analysis

161 Samples of stream water for the routine observation were transported to the
162 laboratory within 1 hour after being collected manually. Samples for the intensive
163 observation were transported within 1 or 2 weeks after completion of the automatic
164 sampling. All samples were passed through a membrane filter (pore size 0.45 μm) and
165 stored in a refrigerator (4 °C) prior to their chemical analysis.

166 The concentrations of nitrate were measured by ion chromatography (DX-500;
167 Dionex Inc., USA). To determine the stable isotopic compositions of nitrate in the
168 stream water samples, nitrate in each sample was chemically converted to N_2O using a
169 method originally developed to determine the $^{15}\text{N}/^{14}\text{N}$ and $^{18}\text{O}/^{16}\text{O}$ ratios of seawater
170 and freshwater nitrate (McIlvin and Altabet, 2005) that was later modified (Konno et
171 al., 2010; Tsunogai et al., 2011; Yamazaki et al., 2011). In brief, 11 mL of each sample
172 solution was pipetted into a vial with a septum cap. Then, 0.5 g of spongy cadmium
173 was added, followed by 150 μL of a 1 M NaHCO_3 solution. The sample was then shaken
174 for 18-24 h at a rate of 2 cycles s^{-1} . Then, the sample solution (10 mL) was decanted
175 into a different vial with a septum cap. After purging the solution using high-purity
176 helium, 0.4 mL of an azide–acetic acid buffer, which had also been purged using high-
177 purity helium, was added. After 45 min, the solution was alkalized by adding 0.2 mL
178 of 6 M NaOH.

179 Then, the stable isotopic compositions ($\delta^{15}\text{N}$, $\delta^{18}\text{O}$, and $\Delta^{17}\text{O}$) of the N_2O in each vial
180 were determined using the continuous-flow isotope ratio mass spectrometry (CF-IRMS)



181 system at Nagoya University. The analytical procedures performed using the CF-IRMS
182 system were the same as those detailed in previous studies (Hirota et al., 2010; Komatsu
183 et al., 2008). The obtained values of $\delta^{15}\text{N}$, $\delta^{18}\text{O}$, and $\Delta^{17}\text{O}$ for the N_2O derived from the
184 nitrate in each sample were compared with those derived from our local laboratory
185 nitrate standards to calibrate the values of the sample nitrate to an international scale
186 and to correct for both isotope fractionation during the chemical conversion to N_2O and
187 the progress of oxygen isotope exchange between the nitrate derived reaction
188 intermediate and water (ca. 20 %). The local laboratory nitrate standards used for the
189 calibration had been calibrated using the internationally distributed isotope reference
190 materials (USGS-34 and USGS-35). In this study, we adopted the internal standard
191 method (Nakagawa et al., 2013, 2018; Tsunogai et al., 2014) to calibrate the stable
192 isotopic compositions of sample nitrate. In order to calibrate the differences in $\delta^{18}\text{O}$ of
193 H_2O between the samples and those our local laboratory nitrate standards were added
194 for calibration, the $\delta^{18}\text{O}$ values of H_2O in the samples were analyzed as well (Tsunogai
195 et al., 2010, 2011, 2014).

196 To determine whether the conversion rate from nitrate to N_2O was sufficient, the
197 concentration of nitrate in the samples was determined each time we analyzed the
198 isotopic composition using CF-IRMS based on the N_2O^+ or O_2^+ outputs. We adopted
199 the $\delta^{15}\text{N}$, $\delta^{18}\text{O}$, and $\Delta^{17}\text{O}$ values only when the concentration measured via CF-IRMS
200 correlated with the concentration measured via ion chromatography prior to isotope
201 analysis within a difference of 10 %.



We repeated the analysis of $\delta^{15}\text{N}$, $\delta^{18}\text{O}$, and $\Delta^{17}\text{O}$ values for each sample at least three times to attain high precision. All samples had a nitrate concentration of greater than 10 μM , which corresponded to a nitrate quantity greater than 100 nmol in a 10 mL sample. Thus, all isotope values presented in this study have an error (standard error of the mean) better than $\pm 0.2\text{‰}$ for $\delta^{15}\text{N}$, $\pm 0.3\text{‰}$ for $\delta^{18}\text{O}$, and $\pm 0.1\text{‰}$ for $\Delta^{17}\text{O}$.

Nitrite (NO_2^-) in the samples interferes with the final N_2O produced from nitrate because the chemical method also converts NO_2^- to N_2O (McIlvin and Altabet, 2005). Therefore, it is sometimes necessary to remove NO_2^- prior to converting nitrate to N_2O . However, in this study, all the stream and soil water samples analyzed for stable isotopic composition had NO_2^- concentrations lower than the detection limit (0.05 μM). Because the minimum nitrate concentration in the samples was 24.7 μM in this study, the ratios of NO_2^- to nitrate in the samples must be less than 0.2 %. Thus, we skipped the processes for removing NO_2^- .

215

2.5 Calculating of the concentration of unprocessed $\text{NO}_3^-_{\text{atm}}$ in stream water

The $\Delta^{17}\text{O}$ data of nitrate in each sample can be used to estimate the concentration of $\text{NO}_3^-_{\text{atm}}$ ($[\text{NO}_3^-_{\text{atm}}]$) in the stream water samples by applying Eq. (2):

$$[\text{NO}_3^-_{\text{atm}}]/[\text{NO}_3^-] = \Delta^{17}\text{O}/\Delta^{17}\text{O}_{\text{atm}} \quad (2)$$

where $[\text{NO}_3^-_{\text{atm}}]$ and $[\text{NO}_3^-]$ denote the concentration of $\text{NO}_3^-_{\text{atm}}$ and nitrate (total) in each water sample, respectively, and $\Delta^{17}\text{O}_{\text{atm}}$ and $\Delta^{17}\text{O}$ denote the $\Delta^{17}\text{O}$ values of $\text{NO}_3^-_{\text{atm}}$ and nitrate (total) in the stream water sample, respectively. In this study, we



used the average $\Delta^{17}\text{O}$ value of NO_3^- determined at the nearby Sado-Seki monitoring station during the observation from April 2009 to March 2012 ($\Delta^{17}\text{O}_{\text{atm}} = +26.3 \text{ ‰}$; Tsunogai et al., 2016) for $\Delta^{17}\text{O}_{\text{atm}}$ in Eq. (2) to estimate $[\text{NO}_3^-]$ in the stream. We allow for an error range in of 3 ‰ in $\Delta^{17}\text{O}_{\text{atm}}$, in which the factor changes in $\Delta^{17}\text{O}_{\text{atm}}$ from +26.3 ‰ caused by both areal and seasonal variation in the $\Delta^{17}\text{O}$ values of NO_3^- have been considered (Nakagawa et al., 2018; Tsunogai et al., 2016).

229

3 Results

3.1 Variation during the routine observation

During the routine observation, the concentrations of stream nitrate ranged from 35.7 μM to 129.3 μM with the flux-weighted average concentration of 55.6 μM (Fig. 2a), showing little temporal changes from that determined during the past observations from 2013 to 2014 at the same catchment (58.4 μM ; Nakagawa et al., 2018). The variation range also agreed with the past observation done in the same catchment (Kamisako et al., 2008), except for the extraordinarily large concentration (129.3 μM) recorded on 2018/8/31, which exceeded the 2σ of the whole variation range of stream nitrate of our routine observation (Fig. 2a). We will discuss the reason in section 4.1.

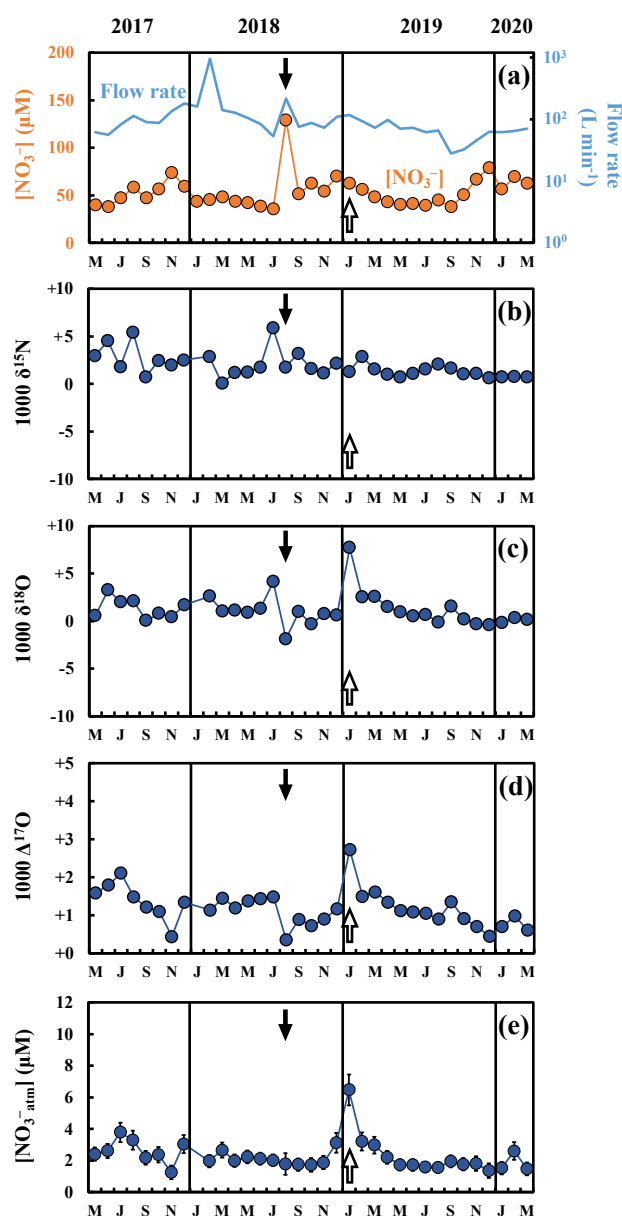
The stable isotopic compositions of stream nitrate during the routine observation ranged from +0.1 ‰ to +5.9 ‰ for $\delta^{15}\text{N}$ (Fig. 2b), from -1.9 ‰ to +7.7 ‰ for $\delta^{18}\text{O}$ (Fig. 2c), and from +0.4 ‰ to +2.7 ‰ for $\Delta^{17}\text{O}$ (Fig. 2d), while showing little seasonal variation. The flux-weighted averages for the $\delta^{15}\text{N}$, $\delta^{18}\text{O}$, and $\Delta^{17}\text{O}$ values of nitrate



244 were +2.0 ‰, +1.1 ‰, and +1.1 ‰, respectively. Except for the extraordinarily large
245 $\delta^{18}\text{O}$ and $\Delta^{17}\text{O}$ values we found on 2019/1/31 ($\delta^{18}\text{O} = +7.7$ ‰ and $\Delta^{17}\text{O} = +2.7$ ‰)
246 (Figs. 2c and 2d), the values are typical for stream nitrate eluted from temperate forested
247 catchments (Hattori et al., 2019; Huang et al., 2020; Nakagawa et al., 2013, 2018; Riha
248 et al., 2014; Sabo et al., 2016; Tsunogai et al., 2014, 2016). On the other hand, the data
249 recorded on 2019/1/31 exceeded the 2σ variation range of the whole $\delta^{18}\text{O}$ and $\Delta^{17}\text{O}$
250 data. We will discuss the reason in section 4.2.



251



252 **Figure 2.** Temporal variations in the concentrations of nitrate (orange circles) and the
 253 flow rates (blue line) in the stream water during the routine observation (a), together
 254 with those of the values of $\delta^{15}\text{N}$ (b), $\delta^{18}\text{O}$ (c), $\Delta^{17}\text{O}$ (d) of nitrate, and the concentrations



255 of unprocessed atmospheric nitrate ($[\text{NO}_3^-]_{\text{atm}}$) (e) in the stream water (blue circles).
 256 The black and white arrows in the figures indicate the sampling that took place on
 257 2018/8/31 and 2019/1/31, respectively. The error bars smaller than the sizes of the
 258 symbols are not presented.

259

260 3.2 Variation in response to the storm events

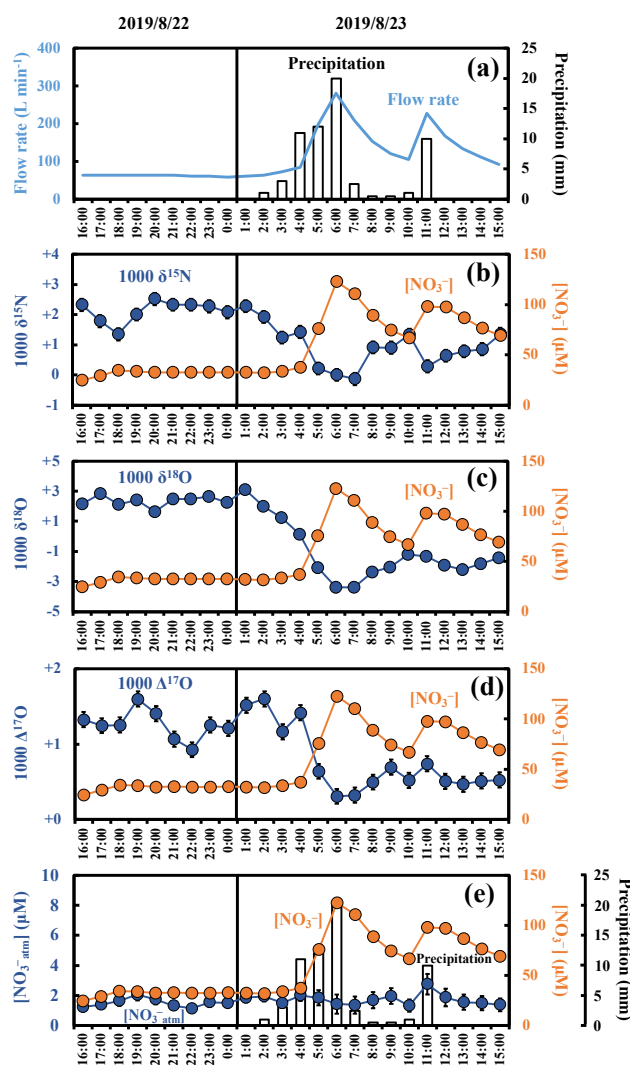
261 During the intensive observations made in response to the storm events, the
 262 concentration of stream nitrate showed significant short-term variation, from 24.7 μM
 263 to 122.6 μM , from 28.7 μM to 134.1 μM , and from 46.6 μM to 114.5 μM during the
 264 storm events I, II, and III, respectively, with the minimum recorded just before the
 265 beginning of each storm event and the maximum recorded when the flow rate was close
 266 to the maximum within each storm event (Figs. 3 and S1). The pattern and range of the
 267 short-term variation of the stream nitrate concentration during the three storm events
 268 were consistent with the past study done in the same catchment (Kamisako et al., 2008).

269 The stable isotopic compositions of stream nitrate during the three storm events also
 270 showed significant temporal variation, from -0.1‰ to $+2.5\text{‰}$, from -0.5‰ to $+3.0\text{‰}$,
 271 and from -0.1‰ to $+3.5\text{‰}$ for $\delta^{15}\text{N}$ (Figs. 3b, S1b, and S1g), from -3.4‰ to $+3.1\text{‰}$,
 272 from -2.5‰ to $+2.9\text{‰}$, and from -2.3‰ to $+2.1\text{‰}$ for $\delta^{18}\text{O}$ (Figs. 3c, S1c, and S1h),
 273 and from $+0.3\text{‰}$ to $+1.6\text{‰}$, from $+0.3\text{‰}$ to $+1.4\text{‰}$, and from $+0.5\text{‰}$ to $+1.2\text{‰}$ for
 274 $\Delta^{17}\text{O}$ (Figs. 3d, S1d, and S1i), with minimum values observed when the concentration
 275 of stream nitrate was at maximum and maximum values observed when the



276 concentration of stream nitrate was at a minimum.

277



278 **Figure. 3** Temporal variations in the precipitation (bar chart) and flow rates (blue line)

279 of the stream water during storm events I (a), together with those in the concentrations

280 of nitrate (orange circles), the values of δ¹⁵N (b), δ¹⁸O (c), Δ¹⁷O (d) of nitrate, and

281 [NO₃⁻]_{atm} (e) in the stream water (blue circles). The error bars smaller than the sizes of



282 the symbols are not presented.

283

284 **4 Discussion**

285 4.1 Primary source of nitrate increased during storm events

286 The striking feature of the observed short-term variation was that all the stable
287 isotopic compositions ($\delta^{15}\text{N}$, $\delta^{18}\text{O}$, and $\Delta^{17}\text{O}$) varied in response to the variation in the
288 nitrate concentration throughout the three storm events (Figs. 3 and S1). The result
289 implied that the source of increased nitrate during the storm events were different from
290 that during the base flow period.

291 The stable isotopic compositions ($\delta^{15}\text{N}$, $\delta^{18}\text{O}$, and $\Delta^{17}\text{O}$) of stream nitrate were
292 plotted as the functions of the reciprocal of the stream nitrate concentration ($1/[\text{NO}_3^-]$)
293 for each storm event (Fig. 4). All the stable isotopic compositions of stream nitrate
294 ($\delta^{15}\text{N}$, $\delta^{18}\text{O}$, and $\Delta^{17}\text{O}$) showed strong linear relationships ($R^2 > 0.5$; $p < 0.001$) with
295 the reciprocal of concentrations. The linear relationships strongly suggest mixing
296 between two endmembers with distinctively different isotopic signatures (e.g.
297 Keeling, 1958). The nitrate-depleted endmember must be the source of stream nitrate
298 during the base flow period prior to each storm event. On the other hand, the nitrate-
299 enriched endmember represents the source of nitrate that was added during the storm
300 events.

301 Atmospheric nitrate ($\text{NO}_3^-_{\text{atm}}$) dissolved in rainwater was one of the possible
302 sources of nitrate enriched during the storm events (Kaushal et al., 2011; Sebestyen et



al., 2014). While the $\text{NO}_3^-_{\text{atm}}$ showed the $\delta^{18}\text{O}$ and $\Delta^{17}\text{O}$ values enriched in both ^{18}O and ^{17}O , more than +55 ‰ and more than +18 ‰, respectively, during summer periods in Japan (Tsunogai et al., 2016), the nitrate-enriched endmember showed the $\delta^{18}\text{O}$ and $\Delta^{17}\text{O}$ values depleted in both ^{18}O and ^{17}O , less than +3.1 ‰ and +1.6 ‰, respectively, during the storm events. The concentrations of $\text{NO}_3^-_{\text{atm}}$ ($[\text{NO}_3^-_{\text{atm}}]$) showed little temporal variations showing the concentrations of $1.6 \pm 0.4 \mu\text{M}$, $1.8 \pm 0.4 \mu\text{M}$, and $2.1 \pm 0.4 \mu\text{M}$ during the storm events I, II, and III, respectively (Figs. 3e, S1e, and S1j). In general, the $[\text{NO}_3^-_{\text{atm}}]$ in rainwater were much higher than those in stream water (Nakagawa et al., 2018; Rose et al., 2015; Tsunogai et al., 2014). During the storm events I, II, and III, however, the $[\text{NO}_3^-_{\text{atm}}]$ in stream water was almost constant irrespective to the increase in precipitation (Figs. 3e, S1e, and S1j). Thus, we conclude that the direct input of $[\text{NO}_3^-_{\text{atm}}]$ via rainwater into the stream through overland flow during storm events can be negligible, at least in the KJ catchment. Thus, we concluded that the $\text{NO}_3^-_{\text{atm}}$ should be the minor source of nitrate that increased during the storm events.

Nakagawa et al. (2018) determined the temporal variations in the concentrations (Fig. 5a) and isotopic compositions ($\delta^{15}\text{N}$, $\delta^{18}\text{O}$, and $\Delta^{17}\text{O}$) (Figs. 5b, 5c, and 5d) of soil nitrate dissolved in soil water taken within the same catchment during 2013 to 2014, at the depths of 20 cm and 60 cm of the station SLS (SLS 20 and SLS 60, respectively) and at the depth of 20 cm of the station SMS (SMS 20), where the station SLS was located in the riparian zone of the stream and the station SMS was



about 20 m away from the stream and located in the upland zone (Fig. 1b). The concentrations of soil nitrate showed significant seasonal variation, with the higher concentration in summer and the lower concentration in winter (Fig. 5a). Both the $\delta^{18}\text{O}$ and $\Delta^{17}\text{O}$ values also showed significant seasonal variation, with the minimum in summer and the maximum in winter (Figs. 5c and d). To verify if the soil nitrate is the source of the stream nitrate that was added to the stream during the storm events, we also plotted soil nitrate at each site (SLS 20, SLS 60 and SMS 20) of the same season in Fig. 4. Because our intensive observations on the storm events were done in summer (from August to October), the average concentration and the average isotopic composition during summer (from August to October) were calculated (Table 1) and plotted in Fig. 4. The error bars of each soil nitrate denote the standard deviation (SD) of each isotopic composition ($n=5$ for each). We found that the isotopic compositions ($\delta^{15}\text{N}$, $\delta^{18}\text{O}$, and $\Delta^{17}\text{O}$) of soil nitrate in the riparian zone (SLS 20 and SLS 60; Table 1) were always plotted on the nitrate-enriched extension (lower $1/[\text{NO}_3^-]$ extension) of the mixing line during the storm events I, II, and III (Fig. 4), while those of the soil nitrate in the upland zone (SMS 20; Table 1) were somewhat deviated from the nitrate-enriched extension of the mixing line, $\delta^{18}\text{O}$ especially (Figs. 4d, 4e, and 4f). We conclude that the primary source of nitrate added during the storm events was the soil nitrate in the riparian zone.

The “flushing hypothesis” has been proposed to explain the increase in stream nitrate concentration in accordance with the increase in flow rate during storm events



345 (Creed et al., 1996; Hornberger et al., 1994). During the base flow periods, nitrate
346 accumulate in shallow, oxic soil layers due to the progress of nitrification. When
347 water level became higher during storm periods, concentration of stream nitrate
348 increased due to flushing of the soil nitrate accumulated in the shallow soil layers of
349 riparian zones into stream (Chen et al., 2020; Creed et al., 1996; Ocampo et al., 2006).
350 Our finding that the primary source of nitrate increased during the storm events was
351 the soil nitrate in the riparian zone is consistent with the “flushing hypothesis.” We
352 conclude that the flushing of soil nitrate in the riparian zone into the stream due to
353 rising of both stream water and groundwater level was responsible for the increase in
354 stream nitrate during the storm events (Fig. 6).

355 Within the whole dataset on the variation of the concentration of nitrate in the stream
356 determined by Kamisako et al. (2008), an increase in the concentration of nitrate in the
357 stream of more than 20 μM in response to storm events was found to be limited to the
358 storm events that occurred in the warm seasons, from June to November. As the
359 concentrations of soil nitrate in the riparian zone (SLS 20 and SLS 60) were much
360 higher in the warm seasons ($734 \mu\text{M} \pm 496 \mu\text{M}$; from June to November) than in the
361 cold seasons ($156 \pm 124 \mu\text{M}$; from December to May), such seasonal variation in the
362 concentration of riparian soil nitrate is consistent with the observed seasonality in the
363 influence of storm events on the stream nitrate concentration, where significant effects
364 are observed during warm months, whereas insignificant effects are observed during
365 cold months.



366 As mentioned in section 3.1, we found significant increase in nitrate concentration
367 up to 129.3 μM on 2018/8/31 during our routine observation on the stream, when the
368 water was sampled in the middle of a heavy storm (59.5 mm per day) with significant
369 increase in flow rate (from 53.4 L/min one month before to 216.9 L/min during
370 sampling). The measured $\delta^{18}\text{O}$ and $\Delta^{17}\text{O}$ value of the stream nitrate on 2018/8/31
371 (-1.9‰ and $+0.4\text{‰}$, respectively) showing significantly smaller values than those
372 during the other routine observation (Fig. 2c and 2d), agreed well with those of the
373 nitrate increase during the storm events I, II, and III. Moreover, both the range of
374 increase in stream nitrate concentration (129.3 μM) and the season of observation
375 (August) also agreed well with those of the stream nitrate increase during the three
376 storm events. As a result, we conclude that the input of soil nitrate accumulated in the
377 riparian zone due to flushing was also responsible for the significant increase in
378 stream nitrate concentration we found on 2018/8/31 during the routine observation.

379

380

381

382

383

384

385

386

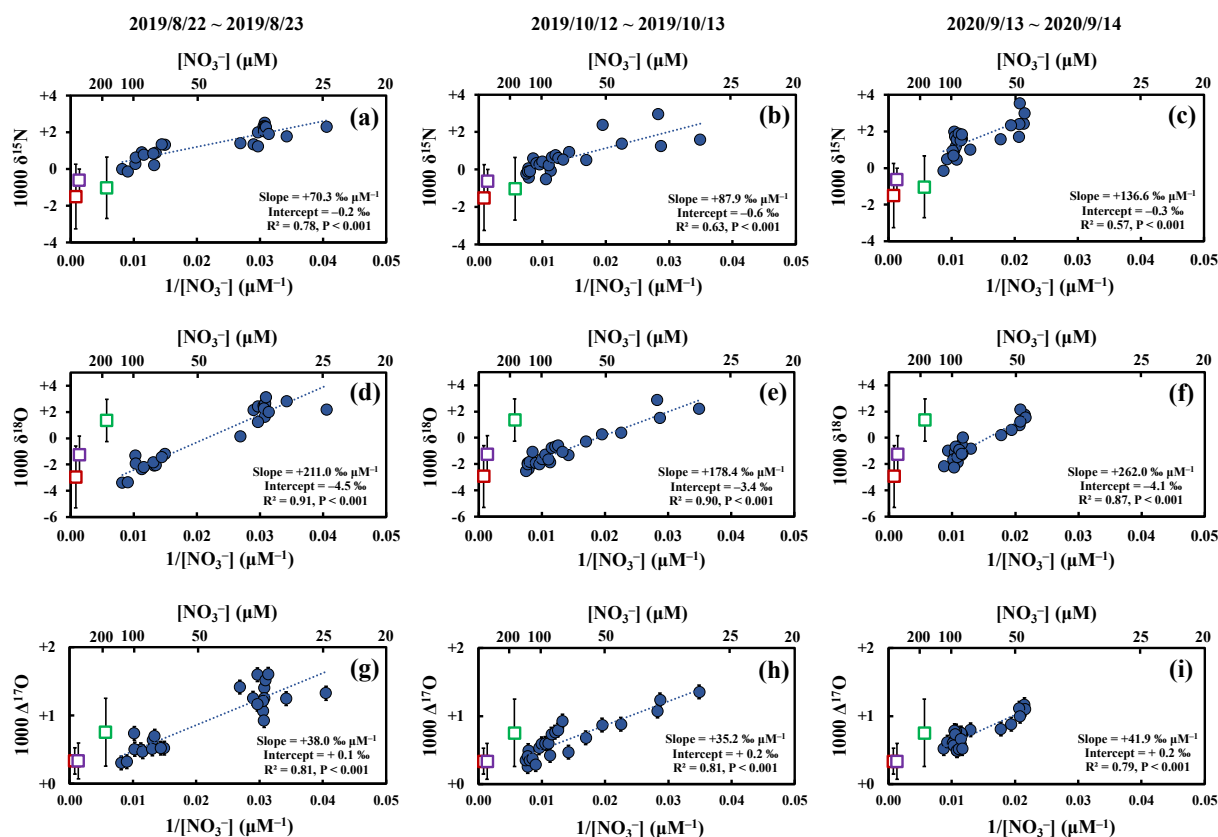


Figure 4. The $\delta^{15}N$ (a, b, and c), $\delta^{18}O$ (d, e, and f), and $\Delta^{17}O$ (g, h, and i) values of stream nitrate (blue circles) during storm events I, II, and III plotted as a function of the reciprocal of nitrate concentration ($1/[NO_3^-]$), together with those of soil nitrate at SLS 20 (red squares), SLS 60 (purple squares), and SMS 20 (green squares) during August to October in 2013 and 2014. The error bars of each soil nitrate denote the standard deviation (SD) of each isotopic composition ($n=5$ for each). The error bars smaller than the sizes of the symbols are not presented.

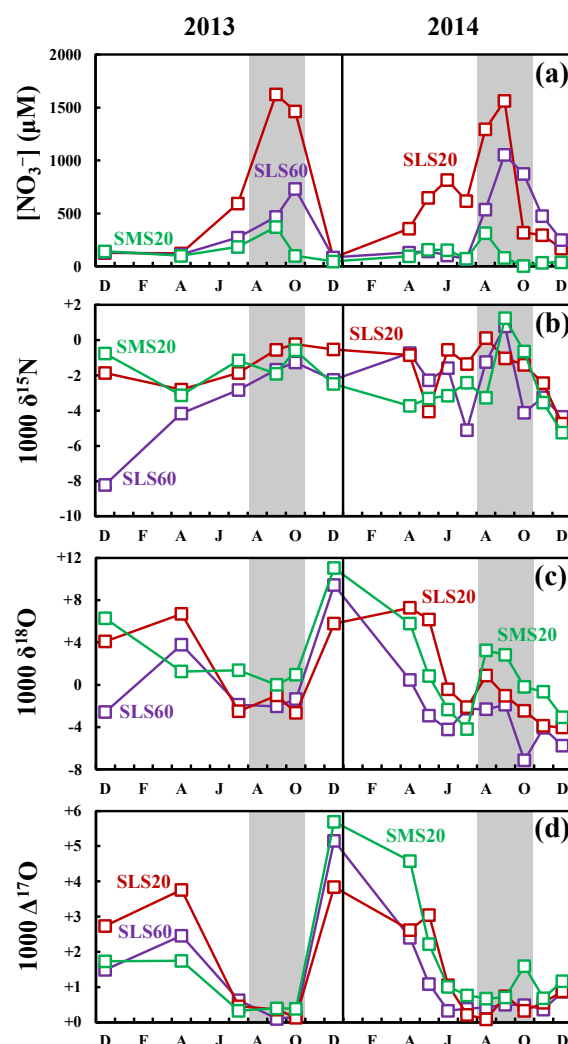
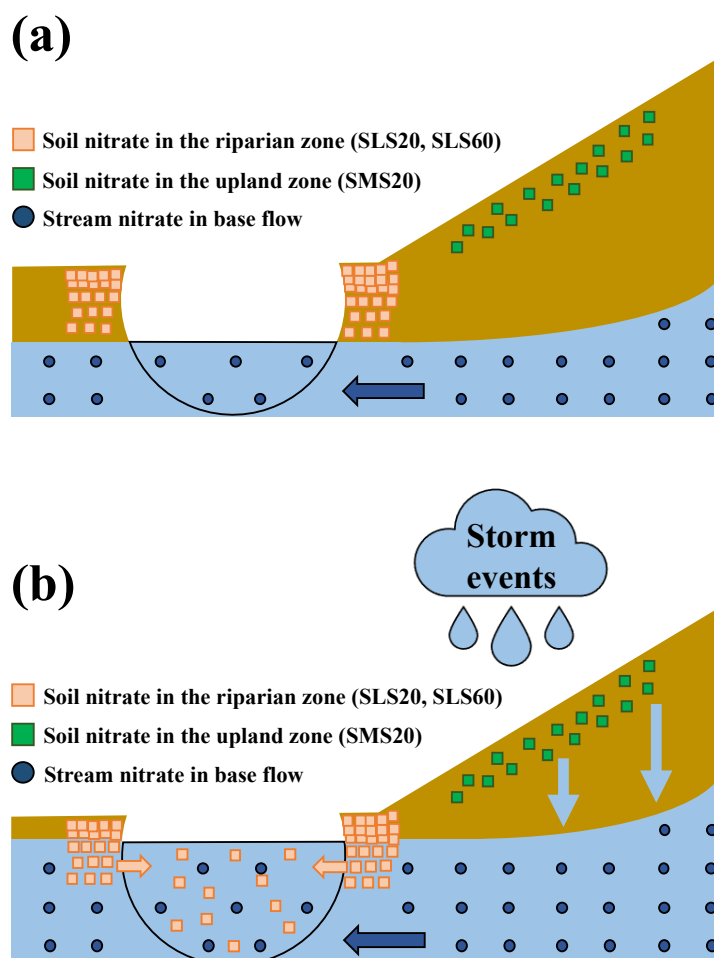


Figure 5. Seasonal variations in the concentrations of soil nitrate (a) at SLS 20 (red squares), SLS 60 (purple squares), and SMS20 (green squares), together with those in the values of $\delta^{15}N$ (b), $\delta^{18}O$ (c) and $\Delta^{17}O$ (d) of each soil nitrate during 2013 to 2014 (modified from Nakagawa et al., 2018). The periods used to estimate the isotopic compositions (from August to October) are presented in gray. The error bars were smaller than the sizes of the symbols.



Table 1 Concentrations and isotopic compositions ($\delta^{15}\text{N}$, $\delta^{18}\text{O}$, and $\Delta^{17}\text{O}$) of soil nitrate at SLS 20, SLS 60, and SMS 20 during August to October in 2013 and 2014 (recalculated from the data in Nakagawa et al., 2018).

	SLS 20	SLS 60	SMS 20
NO_3^- (μM)	1254 ± 537	734 ± 241	176 ± 159
$1000 \delta^{15}\text{N}$	-1.5 ± 1.8	-0.6 ± 0.6	-1.0 ± 1.7
$1000 \delta^{18}\text{O}$	-2.9 ± 2.4	-1.3 ± 1.4	$+1.4 \pm 1.6$
$1000 \Delta^{17}\text{O}$	$+0.3 \pm 0.2$	$+0.3 \pm 0.3$	$+0.8 \pm 0.5$





408 **Figure 6.** Schematic diagram showing the elution of soil nitrate to the stream before
 409 the storm events (a) and during the storm events (b). Soil nitrate in the riparian zone
 410 and that in the upland zone are represented by the orange squares and green squares,
 411 respectively, while stream nitrate during base flow is represented by the blue circles.

412

413 4.2 Variation in the concentration of $\text{NO}_3^-_{\text{atm}}$ during routine observation

414 The concentration of $\text{NO}_3^-_{\text{atm}}$ ($[\text{NO}_3^-_{\text{atm}}]$) showed little seasonal variation, from 1.3
 415 μM to 3.8 μM during our routine observation in this study (Fig. 2e), except for the
 416 extraordinarily large $[\text{NO}_3^-_{\text{atm}}]$ we found on 2019/1/31 (6.5 μM). Except for the
 417 extraordinarily large $[\text{NO}_3^-_{\text{atm}}]$, the obtained $[\text{NO}_3^-_{\text{atm}}]$ corresponded well with those
 418 determined in the past study done at the same catchment (Nakagawa et al., 2018). In
 419 addition, they corresponded well with those of the temperate forested catchments
 420 saturated in nitrogen, such as Qingyuan Forest (2.0 μM ; Huang et al., 2020) and Fernow
 421 experimental Forest 1, 2, and 3 (1.6 μM , 3.4 μM , and 4.2 μM , respectively; Rose et al.,
 422 2015).

423 In this study, accumulation of snow was observed at the KJ catchment on 2019/1/27,
 424 of up to 18 cm, while most of the accumulated snow had melted to a depth of 1 cm
 425 depth by 2019/1/30, prior to the sampling being carried out on 2019/1/31. Furthermore,
 426 during the routine observation period from 2017/5 to 2020/3, no other snow-melting
 427 events were experienced within 4 days prior to the sampling day, except for the
 428 sampling on 2019/1/31. Similar enhancement in the concentration of $\text{NO}_3^-_{\text{atm}}$, as well



429 as the $\delta^{18}\text{O}$ and $\Delta^{17}\text{O}$ of stream nitrate, in response to snow melting has been frequently
430 observed in streams worldwide (Ohte et al., 2004, 2010; Pellerin et al., 2012; Piatek et
431 al., 2005; Rose et al., 2015; Sabo et al., 2016; Tsunogai et al., 2014, 2016). We conclude
432 that input of the $\text{NO}_3^-_{\text{atm}}$ accumulated in the melted snow water, showing $\delta^{18}\text{O}$ and $\Delta^{17}\text{O}$
433 values significantly higher than those in the stream, caused the extraordinarily increase
434 in $[\text{NO}_3^-_{\text{atm}}]$ on 2019/1/31. Except for the extraordinarily increase in $[\text{NO}_3^-_{\text{atm}}]$ ($n = 1$),
435 $[\text{NO}_3^-_{\text{atm}}]$ was stable at $2.2 \pm 0.6 \mu\text{M}$ throughout the routine observation ($n = 33$). We
436 concluded that $[\text{NO}_3^-_{\text{atm}}]$ was generally stable in the stream.

437

438 4.3 The impact of storm events on the index of the nitrogen saturation

439 The concentration of stream nitrate eluted from a forested catchment has been used
440 as an index to evaluate the stage of nitrogen saturation in the forest (Huang et al., 2020;
441 Rose et al., 2015; Stoddard, 1994). However, McHale et al. (2002) pointed out the
442 problem in the reliability of this index, because the number of storm events influenced
443 the concentration of nitrate eluted from forested stream significantly. That is, if we use
444 the concentration of stream nitrate sampled during the storm events to evaluate the stage
445 of nitrogen saturation in a forested catchment, the stage of nitrogen saturation might be
446 overestimated.

447 Nakagawa et al. (2018) have proposed the export flux of $\text{NO}_3^-_{\text{atm}}$ (M_{atm}) relative to
448 the deposition flux of $\text{NO}_3^-_{\text{atm}}$ (D_{atm}) can be an alternative, more robust index for
449 nitrogen saturation in temperate forested catchments. To estimate reliable M_{atm} in each



450 forested catchment, we must obtain reliable $[\text{NO}_3^-]_{\text{atm}}$ in the forested stream, including
 451 their temporal variation. While the past studies focused on the seasonal variation of
 452 concentration and export flux of NO_3^- in forested streams (Hattori et al., 2019;
 453 Nakagawa et al., 2018; Rose et al., 2015; Sabo et al., 2016; Tsunogai et al., 2014), we
 454 had little knowledge on the variation of $[\text{NO}_3^-]_{\text{atm}}$ in response to the increase in nitrate
 455 concentration during storm events prior to this study.

456 As already presented in section 4.1, we found that $[\text{NO}_3^-]_{\text{atm}}$ remained almost
 457 constant irrespective to the significant variation in $[\text{NO}_3^-]$ during storm events (Figs.
 458 3e, S1e, and S1j). Furthermore, during our routine observation on 2018/8/31, the
 459 $[\text{NO}_3^-]_{\text{atm}}$ remained almost constant as well, while $[\text{NO}_3^-]$ increased from 35.7 μM (1
 460 month before) to 129.3 μM (Fig. 2e). The observed $[\text{NO}_3^-]_{\text{atm}}$ showing almost constant
 461 values implies that the primary source of NO_3^- in stream water during storm events
 462 was the NO_3^- stored in groundwater, which is the same source as that during the base
 463 flow periods, rather than the direct input of NO_3^- from rainwater through overland
 464 flow. Hence, on the basis of the data of the annual average flow rate of the stream from
 465 the catchment, a reliable annual M_{atm} can be estimated from $[\text{NO}_3^-]_{\text{atm}}$, even if the
 466 $[\text{NO}_3^-]_{\text{atm}}$ data during storm events is included. While the annual M_{atm} could increase
 467 in response to the increase in the number of storm events because of the increase in the
 468 flow rate, the annual D_{atm} also increases in response to the increase in the number of
 469 storm events. Consequently, it can be concluded that storm events have little impact on
 470 the $M_{\text{atm}}/D_{\text{atm}}$. As long as NO_3^- experiences the metabolized processes (uptake or



denitrification) in forested catchment subsequent to deposition, the $M_{\text{atm}}/D_{\text{atm}}$ can correctly reflect the total demand on $\text{NO}_3^-_{\text{atm}}$ in each forested catchment and thus the nitrogen saturation status. We conclude that the $M_{\text{atm}}/D_{\text{atm}}$ ratio can be used as the robust index to evaluate nitrogen saturation in forested catchments, on which storm events have little influence.

5 Conclusions

Temporal variation in the concentrations and stable isotopic compositions ($\delta^{15}\text{N}$, $\delta^{18}\text{O}$, and $\Delta^{17}\text{O}$) of stream nitrate were determined during storm events to clarify the source of stream nitrate increased during storm events. Because the stable isotopic compositions of soil nitrate in riparian zone during summer agreed well with those of the nitrate-enrich endmember of the stream nitrate during storm events, we conclude that the soil nitrate in riparian zone was responsible for the stream nitrate increased during storm events. Additionally, the concentration of $\text{NO}_3^-_{\text{atm}}$ in stream was almost constant during the storm events, implied that the source of $\text{NO}_3^-_{\text{atm}}$ in stream water during storm events was the $\text{NO}_3^-_{\text{atm}}$ stored in groundwater. We concluded that the number of storm events have little impact on $M_{\text{atm}}/D_{\text{atm}}$ ratio, the index of nitrogen saturation. In addition, the $\Delta^{17}\text{O}$ of nitrate can be applicable as the tracer to clarify the source of nitrate.

Data availability. All the primary data are presented in the Supplement. The other data



492 are available upon request to the corresponding author (Weitian Ding).

493

494 *Author contributions.* WD, UT, NY, and HS designed the study. HY, MM, and HS
495 performed the field observations. HY, MM, and HS determined the concentrations of
496 the samples. WD determined the isotopic compositions of the samples. WD, TS, FN,
497 and UT performed data analysis, and WD and UT wrote the paper with input from MM,
498 HY and HS.

499

500 *Competing interests.* The authors declare that they have no conflict of interest.

501

502 *Acknowledgements.*

503 The samples analyzed in this study were collected through the Long-term
504 Monitoring of Transboundary Air Pollution and Acid Deposition by the Ministry of
505 the Environment in Japan. The authors are grateful to Ryo Shingubara, Masanori Ito,
506 Hao Xu, Hui Lan, Peng Lai, Tianzheng Huang, Yuhei Morishita, Tae Ito, Yuka
507 Tadachi and other present and past members of the Biogeochemistry Group, Nagoya
508 University, for their valuable support throughout this study. This work was supported
509 by a Grant-in-Aid for Scientific Research from the Ministry of Education, Culture,
510 Sports, Science, and Technology of Japan under grant numbers JP17H00780,
511 JP19H04254, and JP19H00955 and by the Yanmar Environmental Sustainability
512 Support Association.



513

514 **Reference**

515 Aber, J. D., Nadelhoffer, K. J., Steudler, P. and Melillo, J. M.: Nitrogen Saturation in
 516 Northern Forest Ecosystems, *Bioscience*, 39(6), 378–386, doi:10.2307/1311067,
 517 1989.

518 Aguilera, R. and Melack, J. M.: Concentration-Discharge Responses to Storm Events
 519 in Coastal California Watersheds, *Water Resour. Res.*, 54(1), 407–424,
 520 doi:10.1002/2017WR021578, 2018.

521 Alexander, B., Hastings, M. G., Allman, D. J., Dachs, J., Thornton, J. A. and
 522 Kunasek, S. A.: Quantifying atmospheric nitrate formation pathways based on a
 523 global model of the oxygen isotopic composition ($\delta^{17}\text{O}$) of atmospheric nitrate,
 524 *Atmos. Chem. Phys.*, 9(14), 5043–5056, doi:10.5194/acp-9-5043-2009, 2009.

525 Burns, D. A. and Kendall, C.: Analysis of $\delta^{15}\text{N}$ and $\delta^{18}\text{O}$ to differentiate NO_3^- sources
 526 in runoff at two watersheds in the Catskill Mountains of New York, *Water Resour.*
 527 *Res.*, 38(5), 91–912, doi:10.1029/2001wr000292, 2002.

528 Chen, X., Tague, C. L., Melack, J. M. and Keller, A. A.: Sensitivity of nitrate
 529 concentration-discharge patterns to soil nitrate distribution and drainage properties in
 530 the vertical dimension, *Hydrol. Process.*, 34(11), 2477–2493, doi:10.1002/hyp.13742,
 531 2020.

532 Creed, I. F., Band, L. E., Foster, N. W., Morrison, I. K., Nicolson, J. A., Semkin, R. S.
 533 and Jeffries, D. S.: Regulation of nitrate-N release from temperate forests: A test of



534 the N flushing hypothesis, *Water Resour. Res.*, 32(11), 3337–3354,
 535 doi:10.1029/96WR02399, 1996.

536 Durka, W., Schulze, E., Gebauer, G. and Voerkeliust, S.: Effects of forest decline on
 537 uptake and leaching of deposited nitrate determined from ^{15}N and ^{18}O measurements,
 538 *Nature*, 372, 765–767, doi: <https://doi.org/10.1038/372765a0>, 1994.

539 Galloway, J. N., Aber, J. D., Erisman, J. W., Seitzinger, S. P., Howarth, R. W.,
 540 Cowling, E. B. and Cosby, B. J.: The nitrogen cascade, *Bioscience*, 53(4), 341–356,
 541 doi:10.1641/0006-3568(2003)053[0341:TNC]2.0.CO;2, 2003.

542 Hattori, S., Nuñez Palma, Y., Itoh, Y., Kawasaki, M., Fujihara, Y., Takase, K. and
 543 Yoshida, N.: Isotopic evidence for seasonality of microbial internal nitrogen cycles in
 544 a temperate forested catchment with heavy snowfall, *Sci. Total Environ.*, 690, 290–
 545 299, doi:10.1016/j.scitotenv.2019.06.507, 2019.

546 Hirota, A., Tsunogai, U., Komatsu, D. D. and Nakagawa, F.: Simultaneous
 547 determination of $\delta^{15}\text{N}$ and $\delta^{18}\text{O}$ of N_2O and $\delta^{13}\text{C}$ of CH_4 in nanomolar quantities from
 548 a single water sample, *Rapid Commun. Mass Spectrom.*, 24, 1085–1092,
 549 doi:10.1002/rcm.4483, 2010.

550 Hornberger, G. M., Bencala, K. E. and McKnight, D. M.: Hydrological controls on
 551 dissolved organic carbon during snowmelt in the Snake River near Montezuma,
 552 *Colorado, Biogeochemistry*, 25(3), 147–165, doi:10.1007/BF00024390, 1994.

553 Huang, S., Wang, F., Elliott, E. M., Zhu, F., Zhu, W., Koba, K., Yu, Z., Hobbie, E.
 554 A., Michalski, G., Kang, R., Wang, A., Zhu, J., Fu, S. and Fang, Y.: Multiyear



555 Measurements on $\Delta^{17}\text{O}$ of Stream Nitrate Indicate High Nitrate Production in a
 556 Temperate Forest, Environ. Sci. Technol., 54(7), 4231–4239,
 557 doi:10.1021/acs.est.9b07839, 2020.

558 Inoue, T., Nakagawa, F., Shibata, H. and Tsunogai, U.: Vertical Changes in the Flux
 559 of Atmospheric Nitrate From a Forest Canopy to the Surface Soil Based on $\Delta^{17}\text{O}$
 560 Values, J. Geophys. Res. Biogeosciences, 126(4), 1–18, doi:10.1029/2020JG005876,
 561 2021.

562 Kaiser, J., Hastings, M. G., Houlton, B. Z., Röckmann, T. and Sigman, D. M.: Triple
 563 oxygen isotope analysis of nitrate using the denitrifier method and thermal
 564 decomposition of N_2O , Anal. Chem., 79(2), 599–607, doi:10.1021/ac061022s, 2007.

565 Kamisako, M., Sase, H., Matsui, T., Suzuki, H., Takahashi, A., Oida, T., Nakata, M.,
 566 Totsuka, T. and Ueda, H.: Seasonal and annual fluxes of inorganic constituents in a
 567 small catchment of a Japanese cedar forest near the sea of Japan, Water. Air. Soil
 568 Pollut., 195(1–4), 51–61, doi:10.1007/s11270-008-9726-8, 2008.

569 Kaushal, S. S., Groffman, P. M., Band, L. E., Elliott, E. M., Shields, C. A. and
 570 Kendall, C.: Tracking nonpoint source nitrogen pollution in human-impacted
 571 watersheds, Environ. Sci. Technol., 45(19), 8225–8232, doi:10.1021/es200779e,
 572 2011.

573 Keeling, D.: The concentration and isotopic abundances of atmospheric carbon
 574 dioxide in rural areas, Geochim. Cosmochim. Acta, 13, 322–334,
 575 doi:https://doi.org/10.1016/0016-7037(58)90033-4, 1958.



- 576 Kendall, C., Elliott, E. M. and Wankel, S. D.: Tracing Anthropogenic Inputs of
 577 Nitrogen to Ecosystems, *Stable Isot. Ecol. Environ. Sci.* Second Ed., 375–449,
 578 doi:10.1002/9780470691854.ch12, 2008.
- 579 Komatsu, D. D., Ishimura, T., Nakagawa, F. and Tsunogai, U.: Determination of the
 580 $^{15}\text{N}/^{14}\text{N}$, $^{17}\text{O}/^{16}\text{O}$, and $^{18}\text{O}/^{16}\text{O}$ ratios of nitrous oxide by using continuous-flow
 581 isotope-ratio mass spectrometry Daisuke, *Rapid Commun. Mass Spectrom.*, 22, 1587–
 582 1596, doi:10.1002/rcm.3493, 2008.
- 583 Konno, U., Tsunogai, U., Komatsu, D. D., Daita, S., Nakagawa, F., Tsuda, A.,
 584 Matsui, T., Eum, Y. J. and Suzuki, K.: Determination of total N_2 fixation rates in the
 585 ocean taking into account both the particulate and filtrate fractions, *Biogeosciences*,
 586 7(8), 2369–2377, doi:10.5194/bg-7-2369-2010, 2010.
- 587 McHale, M. R., McDonnell, J. J., Mitchell, M. J. and Cirimo, C. P.: A field-based
 588 study of soil water and groundwater nitrate release in an Adirondack forested
 589 watershed, *Water Resour. Res.*, 38(4), 2-1-2–16, doi:10.1029/2000wr000102, 2002.
- 590 McIlvin, M. R. and Altabet, M. A.: Chemical conversion of nitrate and nitrite to
 591 nitrous oxide for nitrogen and oxygen isotopic analysis in freshwater and seawater,
 592 *Anal. Chem.*, 77(17), 5589–5595, doi:10.1021/ac050528s, 2005.
- 593 Michalski, G., Scott, Z., Kabling, M. and Thiemens, M. H.: First measurements and
 594 modeling of $\Delta^{17}\text{O}$ in atmospheric nitrate, *Geophys. Res. Lett.*, 30(16), 3–6,
 595 doi:10.1029/2003GL017015, 2003.
- 596 Michalski, G., Meixner, T., Fenn, M., Hernandez, L., Sirulnik, A., Allen, E. and



597 Thiemens, M.: Tracing Atmospheric Nitrate Deposition in a Complex Semiarid
 598 Ecosystem Using $\Delta^{17}\text{O}$, *Environ. Sci. Technol.*, 38(7), 2175–2181,
 599 doi:10.1021/es034980+, 2004.

600 Mitchell, M. J., Iwatsubo, G., Ohnishi, K. and Nakagawa, Y.: Nitrogen saturation in
 601 Japanese forests: An evaluation, *For. Ecol. Manage.*, 97(1), 39–51,
 602 doi:10.1016/S0378-1127(97)00047-9, 1997.

603 Morin, S., Sander, R. and Savarino, J.: Simulation of the diurnal variations of the
 604 oxygen isotope anomaly ($\Delta^{17}\text{O}$) of reactive atmospheric species, *Atmos. Chem. Phys.*,
 605 11(8), 3653–3671, doi:10.5194/acp-11-3653-2011, 2011.

606 Nakagawa, F., Suzuki, A., Daita, S., Ohyama, T., Komatsu, D. D. and Tsunogai, U.:
 607 Tracing atmospheric nitrate in groundwater using triple oxygen isotopes: Evaluation
 608 based on bottled drinking water, *Biogeosciences*, 10(6), 3547–3558, doi:10.5194/bg-
 609 10-3547-2013, 2013.

610 Nakagawa, F., Tsunogai, U., Obata, Y., Ando, K., Yamashita, N., Saito, T.,
 611 Uchiyama, S., Morohashi, M. and Sase, H.: Export flux of unprocessed atmospheric
 612 nitrate from temperate forested catchments: A possible new index for nitrogen
 613 saturation, *Biogeosciences*, 15(22), 7025–7042, doi:10.5194/bg-15-7025-2018, 2018.

614 Nelson, D. M., Tsunogai, U., Ding, D., Ohyama, T., Komatsu, D. D., Nakagawa, F.,
 615 Noguchi, I. and Yamaguchi, T.: Triple oxygen isotopes indicate urbanization affects
 616 sources of nitrate in wet and dry atmospheric deposition, *Atmos. Chem. Phys.*, 18(9),
 617 6381–6392, doi:10.5194/acp-18-6381-2018, 2018.



618 Ocampo, C. J., Sivapalan, M. and Oldham, C.: Hydrological connectivity of upland-
 619 riparian zones in agricultural catchments: Implications for runoff generation and
 620 nitrate transport, *J. Hydrol.*, 331(3–4), 643–658, doi:10.1016/j.jhydrol.2006.06.010,
 621 2006.

622 Ohte, N., Sebestyen, S. D., Shanley, J. B., Doctor, D. H., Kendall, C., Wankel, S. D.
 623 and Boyer, E. W.: Tracing sources of nitrate in snowmelt runoff using a high-
 624 resolution isotopic technique, *Geophys. Res. Lett.*, 31(21), 2–5,
 625 doi:10.1029/2004GL020908, 2004.

626 Ohte, N., Tayasu, I., Kohzu, A., Yoshimizu, C., Osaka, K., Makabe, A., Koba, K.,
 627 Yoshida, N. and Nagata, T.: Spatial distribution of nitrate sources of rivers in the lake
 628 Biwa Watershed, Japan: Controlling factors revealed by nitrogen and oxygen isotope
 629 values, *Water Resour. Res.*, 46(7), 1–16, doi:10.1029/2009WR007871, 2010.

630 Paerl, H. W. and Huisman, J.: Climate change: A catalyst for global expansion of
 631 harmful cyanobacterial blooms, *Environ. Microbiol. Rep.*, 1(1), 27–37,
 632 doi:10.1111/j.1758-2229.2008.00004.x, 2009.

633 Pellerin, B. A., Saraceno, J. F., Shanley, J. B., Sebestyen, S. D., Aiken, G. R.,
 634 Wollheim, W. M. and Bergamaschi, B. A.: Taking the pulse of snowmelt: In situ
 635 sensors reveal seasonal, event and diurnal patterns of nitrate and dissolved organic
 636 matter variability in an upland forest stream, *Biogeochemistry*, 108(1–3), 183–198,
 637 doi:10.1007/s10533-011-9589-8, 2012.

638 Peterjohn, W. T., Adams, M. B. and Gilliam, F. S.: Symptoms of nitrogen saturation



639 in two central Appalachian hardwood forest ecosystems, *Biogeochemistry*, 35(3),
 640 507–522, doi:10.1007/BF02183038, 1996.

641 Piatek, K. B., Mitchell, M. J., Silva, S. R. and Kendall, C.: Sources of nitrate in
 642 snowmelt discharge: Evidence from water chemistry and stable isotopes of nitrate,
 643 *Water. Air. Soil Pollut.*, 165(1–4), 13–35, doi:10.1007/s11270-005-4641-8, 2005.

644 Riha, K. M., Michalski, G., Gallo, E. L., Lohse, K. A., Brooks, P. D. and Meixner, T.:
 645 High Atmospheric Nitrate Inputs and Nitrogen Turnover in Semi-arid Urban
 646 Catchments, *Ecosystems*, 17(8), 1309–1325, doi:10.1007/s10021-014-9797-x, 2014.

647 Rose, L. A., Elliott, E. M. and Adams, M. B.: Triple Nitrate Isotopes Indicate
 648 Differing Nitrate Source Contributions to Streams Across a Nitrogen Saturation
 649 Gradient, *Ecosystems*, 18(7), 1209–1223, doi:10.1007/s10021-015-9891-8, 2015.

650 Sabo, R. D., Nelson, D. M. and Eshleman, K. N.: Episodic, seasonal, and annual
 651 export of atmospheric and microbial nitrate from a temperate forest, *Geophys. Res.*
 652 *Lett.*, 43(2), 683–691, doi:10.1002/2015GL066758, 2016.

653 Sase, H., Takahashi, A., Sato, M., Kobayashi, H., Nakata, M. and Totsuka, T.:
 654 Seasonal variation in the atmospheric deposition of inorganic constituents and canopy
 655 interactions in a Japanese cedar forest, *Environ. Pollut.*, 152(1), 1–10,
 656 doi:10.1016/j.envpol.2007.06.023, 2008.

657 Sase, H., Saito, T., Takahashi, M., Morohashi, M., Yamashita, N., Inomata, Y.,
 658 Ohizumi, T. and Nakata, M.: Transboundary air pollution reduction rapidly reflected
 659 in stream water chemistry in forested catchment on the Sea of Japan coast in central



660 Japan, Atmos. Environ., 248(November 2020), 118223,
 661 doi:10.1016/j.atmosenv.2021.118223, 2021.

662 Sebestyen, S. D., Shanley, J. B., Boyer, E. W., Kendall, C. and Doctor, D. H.:
 663 Coupled hydrological and biogeochemical processes controlling variability of
 664 nitrogen species in streamflow during autumn in an upland forest, , 1569–1591,
 665 doi:10.1002/2013WR013670, 2014.

666 Stoddard, J. L.: Long-Term Changes in Watershed Retention of Nitrogen, , 223–284,
 667 doi:10.1021/ba-1994-0237.ch008, 1994.

668 Tsunogai, U., Komatsu, D. D., Daita, S., Kazemi, G. A., Nakagawa, F., Noguchi, I.
 669 and Zhang, J.: Tracing the fate of atmospheric nitrate deposited onto a forest
 670 ecosystem in Eastern Asia using $\Delta^{17}\text{O}$, Atmos. Chem. Phys., 10(4), 1809–1820,
 671 doi:10.5194/acp-10-1809-2010, 2010.

672 Tsunogai, U., Daita, S., Komatsu, D. D., Nakagawa, F. and Tanaka, A.: Quantifying
 673 nitrate dynamics in an oligotrophic lake using $\Delta^{17}\text{O}$, Biogeosciences, 8(3), 687–702,
 674 doi:10.5194/bg-8-687-2011, 2011.

675 Tsunogai, U., Komatsu, D. D., Ohyama, T., Suzuki, A., Nakagawa, F., Noguchi, I.,
 676 Takagi, K. and Nomura, M.: Quantifying the effects of clear-cutting and strip-cutting
 677 on nitrate dynamics in a forested watershed using triple oxygen isotopes as tracers, ,
 678 (1), 5411–5424, doi:10.5194/bg-11-5411-2014, 2014.

679 Tsunogai, U., Miyauchi, T., Ohyama, T., Komatsu, D. D., Nakagawa, F., Obata, Y.,
 680 Sato, K. and Ohizumi, T.: Accurate and precise quantification of atmospheric nitrate



681 in streams draining land of various uses by using triple oxygen isotopes as tracers,
682 Biogeosciences, 13(11), 3441–3459, doi:10.5194/bg-13-3441-2016, 2016.
683 Tsunogai, U., Miyauchi, T., Ohyama, T., Komatsu, D. D., Ito, M. and Nakagawa, F.:
684 Quantifying nitrate dynamics in a mesotrophic lake using triple oxygen isotopes as
685 tracers, Limnol. Oceanogr., 63, S458–S476, doi:10.1002/lno.10775, 2018.
686 Vitousek, P. M. and Howarth, R. W.: Nitrogen limitation on land and in the sea: How
687 can it occur?, Biogeochemistry, 13(2), 87–115, doi:10.1007/BF00002772, 1991.
688 Yamazaki, A., Watanabe, T. and Tsunogai, U.: Nitrogen isotopes of organic nitrogen
689 in reef coral skeletons as a proxy of tropical nutrient dynamics, Geophys. Res. Lett.,
690 38(19), 1–5, doi:10.1029/2011GL049053, 2011.